THE JOURNAL OF PHYSICAL CHEMISTRY C

pubs.acs.org/JPCC Article

Influence of the Chemical Structure on Molecular Light Emission in Strongly Localized Plasmonic Fields

Published as part of The Journal of Physical Chemistry virtual special issue "Toward Chemistry in Real Space and Real Time".

Yao Zhang, Zhen-Chao Dong, and Javier Aizpurua*

Cite This: *J. Phys. Chem. C* 2020, 124, 4674−4683 Read Online

ACCESS | Metrics & More | Article Recommendations | Supporting Information

ABSTRACT: The coupling between a molecular emitter and an optical cavity is often addressed theoretically with the molecule regarded as a point dipole, thus lacking any information on chemical structure. This approximation usually works well because the spatial extent of the electromagnetic fields considered is typically spread over a larger volume than the size of the molecule. However, in extreme plasmonic structures as those used in state-of-the-art nanophotonics, the local electric field is much more confined, producing an inhomogeneous spatial distribution of photonic states reaching 1 nm or less, comparable or even smaller than the molecular size. In such a situation, it is necessary to consider the spatial distribution of the electronic transitions in the molecule to properly describe plasmon-exciton coupling. By introducing the concept of electronic transition current density to describe the excitonic emission from a single molecule, we are able to account for the inhomogeneity of the plasmonic field in the process of light emission and analyze its properties. With the use of this formalism, we address the modification of light emission from a molecule placed at a subnanometer distance from an atomic-scale feature of a plasmonic structure, indicating the failure of the point−dipole approximation and the importance of considering the spatial distribution of both photonic and electronic states.

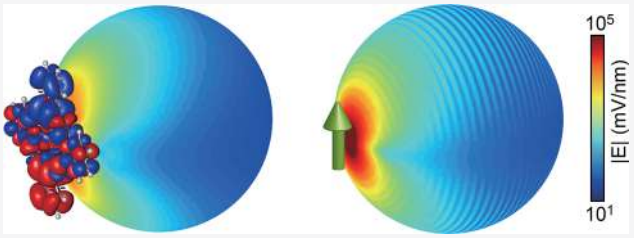

INTRODUCTION

The spontaneous emission rate of a quantum emitter located in an optical resonator can be either enhanced or suppressed depending on the specific location of the emitter, as this emission rate depends on the photonic local density of states (LDOS). This enhancement of the spontaneous emission is known as the Purcell effect.[1,2] The spatial variation of the LDOS usually shows a larger extension than the size of the quantum emitter, and thus the embedded atom, molecule, or quantum dot emitter located in the resonator can be usually regarded as a point dipole.[3−6] This point−dipole approximation is applicable in most conditions when the emitter is located nearby different optical resonators such as Fabry−Perot cavities,[7] microresonators,[8] and photonic crystals cavities.[9] However, recent developments in plasmonic nanoantennas have allowed the local electric field to be confined at the nanoscale,[10] giving rise to the emergence of a new type of optical resonators, so-called "optical nanocavities".[11−14] Furthermore, when light localization occurs even at the atomic scale, concentrated at the subnanometer scale around a few metallic atoms, these structures are referred to as "picocavities".[15] The extension of the light confinement in these extreme nanoantennas and cavities are often comparable to the size of a molecule.[16−21] Under those conditions, the molecule cannot be considered as a point dipole because each distinctive region of the molecule experiences different local fields at their particular position in the cavity, and therefore, the properties of the molecule−cavity coupled system requires one to consider the spatial distribution of both the photonic states in the plasmonic nanoantenna and the excitonic states in the molecule.[16,22−27]

In this context, the light emission from a molecule can be described as the transition between different electronic states which can be accurately calculated within quantum chemistry theory. The spatial distribution of such transition can be addressed through the electronic transition density.[28,29] This transition density provides an electrostatic description that allows for addressing the exciton−polariton coupling including light excitation and emission properties;[27] however, such a description is limited to describe the radiation properties of the molecule−nanoantenna system for situations where retardation in the electromagnetic interaction does not play a relevant

Received: October 31, 2019
Revised: January 9, 2020
Published: January 29, 2020

role. To overcome this issue, and to fully account for retardation in the interaction with the nanoantenna structure, in this work, we introduce the concept of electronic transition current density, complementary to the transition (charge) density. As an example, we apply this formalism to describe the properties of molecular emission from a typical dye molecule, zinc phthalocyanine (ZnPc), close to a spherical metallic nanoantenna whose plasmonic response can be described analytically within Mie theory. By tuning the nanoantenna size and the distance of the molecule to the particle's surface, as well as the relative position between the molecule and the nanoparticle, we find that when the particle size and/or the molecule-particle separation distance are comparable to the size of the molecule, the properties of light emission from the full quantum description introduced here are different from those obtained within the point−dipole approximation. Furthermore, the ZnPc molecule contains two equivalent transition dipoles along two orthogonal directions with the same magnitude, so that if the transition dipole moment is regarded as a point dipole, its associated molecular emission misses the anisotropic features associated with the molecular chemical structure. Recent experimental work on coherent coupling between a single ZnPc molecule and a plasmonic nanocavity, however, reveals that the fluorescence contains information about the symmetry of the molecular structure,[24] an effect that we reproduce here within our full quantum chemistry description of the molecular emitter. This clearly indicates the importance of considering the spatial distribution of the excitonic states when the size of the plasmonic localization is comparable to the size of the molecule. We verify this influence of the molecular structure in a variety of light emission properties including excitation/emission rate, Purcell factor, Lamb shift, and light emission patterns. These results show the importance of a proper combination of quantum chemistry methods with electromagnetic calculations to theoretically address the properties of excitonic emission from molecules in nanoscale plasmonic antennas and cavities.

THEORETICAL MODEL

The light emission from an exciton in a molecule can be related to the dipolar transition between the many-body highest occupied molecular orbital (HOMO) and the lowest unoccupied molecular orbital (LUMO). This electronic transition density ρ_{eg} can be defined from the wave functions of the ground and excited states as $\rho_{eg} = \Psi_e^*(\mathbf{r})\Psi_g(\mathbf{r})$, where $\Psi_e^*(\mathbf{r})$ is the space-dependent wave function of the excited state, and $\Psi_g(\mathbf{r})$ is the wave function of the ground state. The spatial distributions of these wave functions $\Psi_{e(g)}$ can be calculated within the density functional theory (DFT) (see section S1 of Supporting Information for details). To address the optical properties of the coupled molecule-nanoparticle system, we can define a molecular electronic transition current density, $\mathbf{j}_{eg}$,[28,29] also related to the wave functions of the ground and excited states following

$$\mathbf{j}_{eg}(\mathbf{r}) = -\frac{i\hbar}{2m_e}[\Psi_e^*(\mathbf{r})\nabla\Psi_g(\mathbf{r}) - \Psi_g^*(\mathbf{r})\nabla\Psi_e(\mathbf{r})] \quad (1)$$

where $\hbar$ is the Plank constant and m_e is the mass of the electron. The relationship between the transition density ρ_{eg} and the transition current $\mathbf{j}_{eg}$ is given by the continuity equation[30] $\nabla\cdot\mathbf{j}_{eg}(\mathbf{r}) = -\partial\rho_{eg}(\mathbf{r})/\partial t = i\omega_{eg}\rho_{eg}(\mathbf{r})$, where ω_{eg} is the angular frequency associated with the excitonic transition. The transition dipole moment can thus be obtained as $\mu_{eg} = -e\langle\psi_e|\hat{\mathbf{r}}|\psi_g\rangle = -e\int\mathbf{r}\rho_{eg}(\mathbf{r})\,d^3\mathbf{r} = (ie/\omega_{eg})\int\mathbf{j}_{eg}(\mathbf{r})\,d^3\mathbf{r}$ where e is the electron charge. The definition of the electronic transition current allows to obtain the radiative properties of the molecular transition in the presence of a nanoantenna.

Interestingly, the electromagnetic coupling (g) of the molecular dipole to the nanoantenna plasmonic field, can be obtained with the use of the current density, as $g = (-ie/\omega_{eg})\int\mathbf{j}_{eg}(\mathbf{r})\cdot\mathbf{E}(\mathbf{r})\,d^3\mathbf{r}$. This expression of g differs from that based on the transition density,[27] where g is expressed as $g = \int\rho_{eg}(\mathbf{r})\phi(\mathbf{r})\,d^3\mathbf{r}$, with ϕ the scalar potential of the electric field $\mathbf{E} = -\nabla\phi$ (without a well-defined absolute value), and ρ_{eg} is usually expressed in terms of electrostatic charges. Compared to the latter, the expression of the electromagnetic coupling, g, based on the current density shows several advantages, since it involves the direct value of the electric field with no ambiguity, as well as the transition current density itself (or equivalent dipole), which describes the dynamical behavior of the molecular transition. For practical implementation, this current density can be considered to be constituted from conveniently distributed radiating local dipoles, as we discuss below.

As an example of application of this formalism, we consider the electronic structure of the ZnPc molecule which belongs to the D_{4h} point group with "four-lobe" symmetry. Figure 1a shows the chemical structure of this molecule. Two nearly degenerated transitions from the ground electronic state S_0 to two equivalent excited states S_1 and S_2 are found, as schematically shown in Figure 1b, with a transition energy of 2.26 eV. In Figure 1c, the isosurface plots of the electronic transition densities corresponding to these two degenerated transitions are shown based on the DFT calculations (see section S1 of Supporting Information for details). It can be observed that the spatial distributions of $S_0 \rightarrow S_1$ and $S_0 \rightarrow S_2$ transitions are equivalent and the only difference between them is a 90° rotation. Figure 1d shows the spatial distribution of the electronic transition current in a plane above the molecule (red arrows). The flow of the transition current generally follows the direction of the corresponding transition dipole for the two cases considered. In contrast to the electrostatic charge distribution of the transition density, ρ_{eg}, the transition current, $\mathbf{j}_{eg}$, behaves as a radiation source that can interact with the nanoantenna fully considering retardation

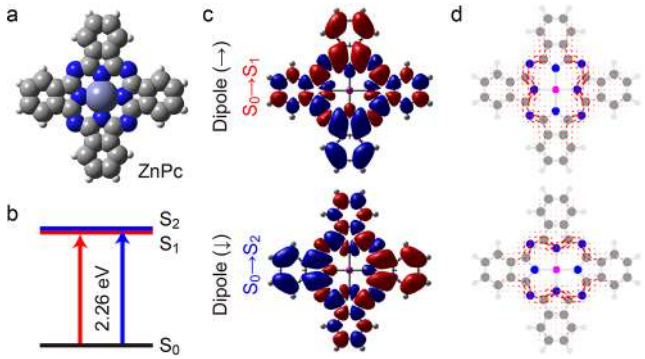

Figure 1. (a) Chemical structure of ZnPc molecule. (b) Energy level diagram of the two degenerated transitions of the ZnPc molecule. (c) Isosurface of the electronic transition densities corresponding to the $S_0 \rightarrow S_1$ and $S_0 \rightarrow S_2$ transitions. (d) Arrow plot of the electronic transition currents of the same transitions as in part c in a plane 0.1 nm above the central molecular plane.

https://dx.doi.org/10.1021/acs.jpcc.9b10256
J. Phys. Chem. C 2020, 124, 4674−4683

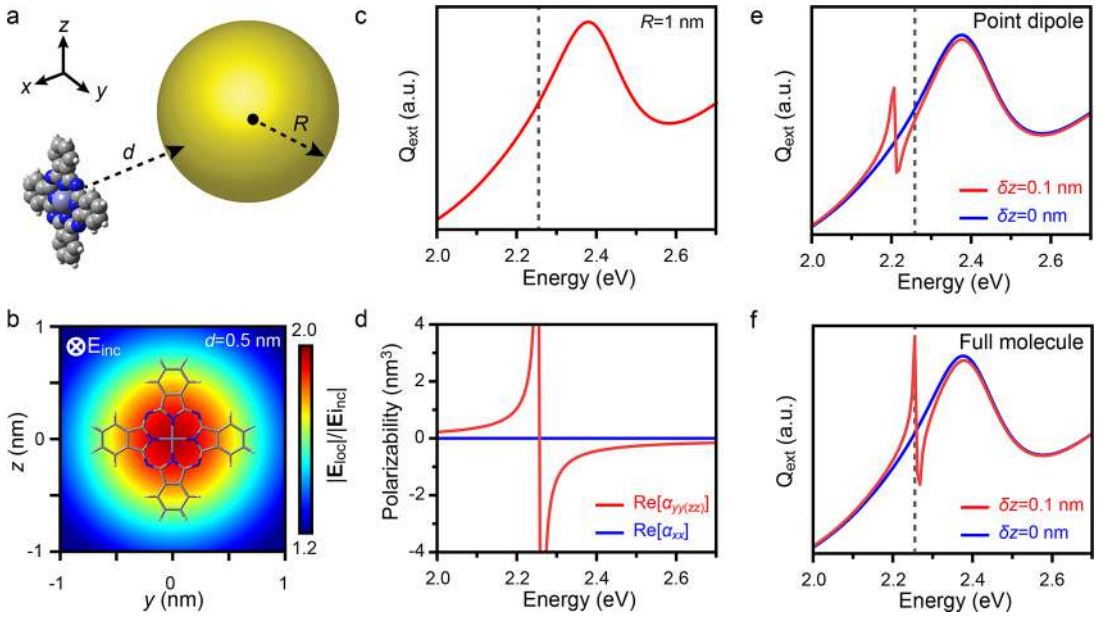

Figure 2. (a) Schematic of the molecule-plasmon coupled system composed by a gold nanoparticle of radius R and a ZnPc molecule at a distance d away from the metal surface. (b) Local electric field distribution for the gold nanoparticle of radius R = 1 nm in the yz plane of the molecule at a distance d = 0.5 nm, excited by a plane wave of energy $\hbar\omega$ = 2.26 eV with polarization perpendicular (along x-axis) to the molecular plane. (c) Extinction spectrum of a gold nanoparticle of radius of R = 1 nm. The transition frequency of the ZnPc molecule is denoted with a dashed line. (d) Real part of the polarizability components Re$\{\alpha_{yy(zz)}\}$ and Re$\{\alpha_{xx}\}$ of the ZnPc molecule. (e, f) Extinction spectra of the molecule−nanoantenna system for the point dipole (e) and full molecule (f) descriptions, respectively. The molecular position is d = 0.5 nm away from the sphere surface, and shifted along the z axis by δz = 0 and 0.1 nm corresponding to the blue and red curves. The molecular transition energy is indicated with the dashed lines.

effects in the interaction. To implement this scheme in the numerical calculations, we further define a set of local dipole moments, $\delta\mu_{eg}^{(j)}$, that play the role of local sources of the transition current $\mathbf{j}_{eg}$ in a small unit volume V_j around position $\mathbf{r}_j$ at the molecule, as $\delta\mu_{eg}^{(j)} = (ie/\omega_{eg})\int_{V_j} \mathbf{j}_{eg}(\mathbf{r})\, d^3\mathbf{r}$. In this way, the molecular transition can be described as a collection of local dipole moments, which can interact with the plasmonic antenna, capturing the main features of this coupling. To show the potential of the method, in the following we address the modification of the properties of excitation and radiation of the ZnPc molecule in the presence of a single metallic nanoparticle acting as a nanoantenna.

RESULTS

Optical Absorption of the Coupled Antenna-Molecule System. Let us consider the ZnPc molecule close to a gold spherical nanoparticle, as shown in Figure 2a, where an effective molecular exciton−plasmon coupling can be produced. The ZnPc molecule shows a planar configuration, assumed to lie in the yz plane. The center of the spherical gold nanoparticle of radius R is located along the x-axis with a separation distance d between the center of the molecule and the particle surface, as depicted in Figure 2a. The optical response of the isolated gold nanoparticle can be calculated using Mie theory, where we apply a maximum angular momentum of l_{max} = 100 in the expansion of the electric field in the vector spherical harmonics (VSHs). We will study here very small metallic nanoparticles, as good representative examples of the class of nanoantennas and nanocavities which show strong field confinement at nanometric and subnanometric scales.[5] In this context, these extremely small particles can be understood as key substructures of larger systems which focus local fields at atomic-scale regions ("hot spots"), such as those present in picocavities,[15,19] for instance. For this reason, nanoparticles as small as 1 nm will be often considered in our study. The extinction spectrum of such an isolated gold nanoparticle of radius R = 1 nm, shown in Figure 2c, exhibits a broad localized dipolar surface plasmonic resonance, centered at around 2.4 eV, typical of gold nanoparticles. Figure 2b shows the local electric near-field distribution $\mathbf{E}_{loc}$ in the yz plane, at a distance d = 0.5 nm from the metallic nanoparticle, excited by a plane wave of frequency ω = 2.26 eV with incident polarization prependicular to this plane, i.e., along the x-axis. As observed, in such a configuration, the local electric near-field resulting from the scattering of the gold nanoparticle exhibits an isotropic distribution in the yz plane (pointing mainly along the x axis). Within this illumination, the molecule is located with its dipole moments μ_y and μ_z lying on this plane, and then the interaction between the nanoantenna local field and any of the two possible molecular dipoles is weak, as plasmonic field and molecular dipoles are almost perpendicular to each other. If the polarization of the incident field, and thus that of its corresponding induced field, were along one of the molecular lobes (for example the transversal z-axis), the $S_0 \rightarrow S_1$ transition in the molecule would be more strongly coupled (with dipole moment μ_z).

Let us consider now the excitation of the ZnPc molecule within the point dipole approximation. The frequency of the incident light is nearly resonant with the electronic transition energy of the molecule. The polarizability tensor of the molecule can be written as[31]

$$\hat{\alpha}_{\mathrm{mol}} = \sum_{n=1,2} \{2\omega_{e_n g}\mu_{g e_n}\mu_{e_n g}/[\hbar(\omega_{e_n g}^2 - \omega^2 - i\omega\gamma_n)]\} \quad (2)$$

https://dx.doi.org/10.1021/acs.jpcc.9b10256
J. Phys. Chem. C 2020, 124, 4674−4683

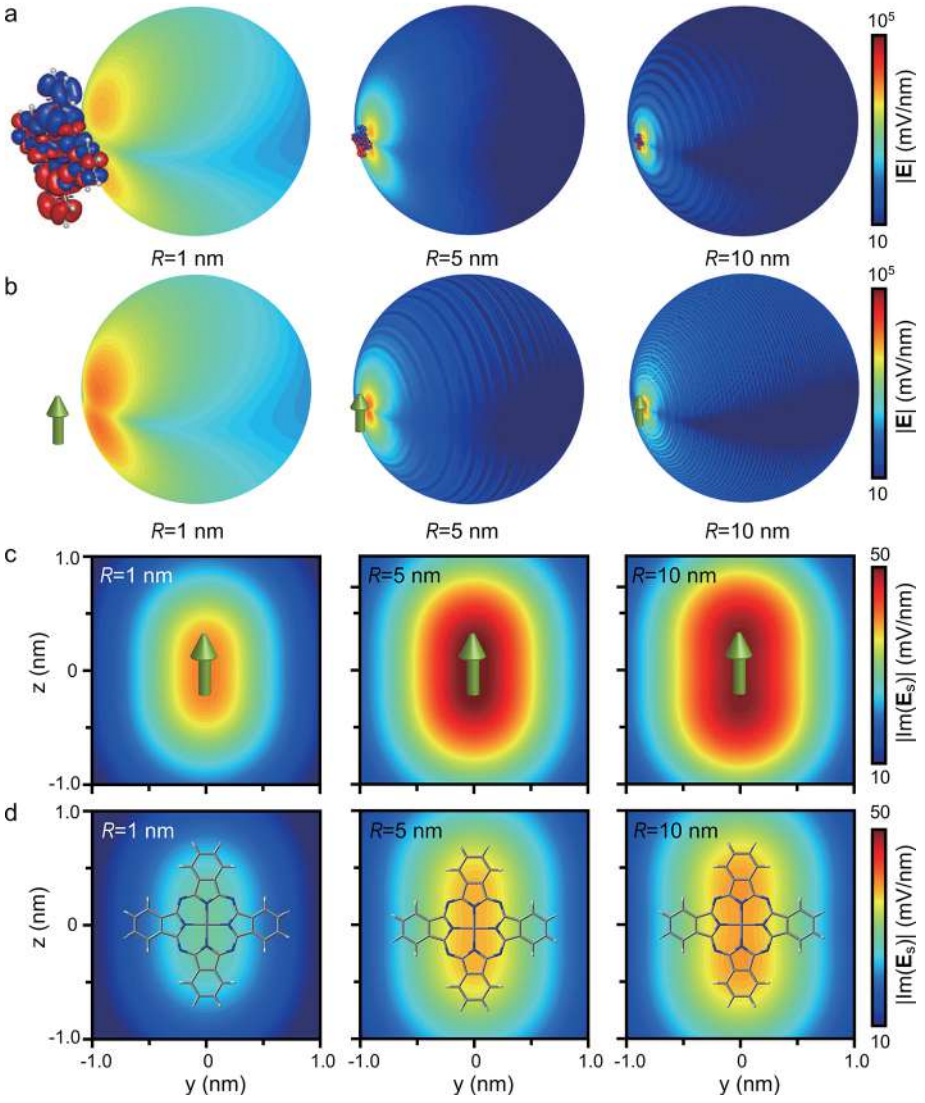

Figure 3. (a, b) Local electric field distributions on the surface of the spherical nanoparticle with different radius: R = 1, 5, and 10 nm excited by a full molecular dipole (a) and by a point dipole (b) at a distance d = 0.5 nm. (c, d) Imaginary part of the corresponding scattering (self-interaction) fields for the point dipole (c) and the full molecular dipole (d) on a molecular plane at a distance d = 0.5 nm. The schematics of the point dipole and the full molecular structure are superimposed to show the relative size of the molecule.

where ω_{e_ng} is the electronic transition frequency, $\mu_{e_ng(ge_n)}$ the transition dipole moment and γ_n the decay rate of the nth excited state (n = 1 for $S_0 \rightarrow S_1$ and n = 2 for $S_0 \rightarrow S_2$). The real part of the molecular polarizability is shown in Figure 2d.

The excitation rate of a molecule within the point-dipole approximation can be obtained by evaluating the electric field experienced by the molecule at that point, as[31]

$$\gamma_{\text{exc}} = \text{Im}[\mathbf{E}^{0*}_{\text{loc}} \cdot \hat{\alpha}_{\text{mol}} \cdot \mathbf{E}^{0}_{\text{loc}}]/2\hbar \tag{3}$$

where $\mathbf{E}^0_{\text{loc}}$ is the local field at the central position of the molecule (point-like), and Im{x} stands for the imaginary part of {x}. For the full description of the molecular transition, however, the description of the excitation rate, γ_{exc}, in the above equation is replaced by an overall integral in space of the local transition dipoles (explicit expressions can be found in section S2 of Supporting Information).

We analyze now the modification of the excitation rate of the molecule due to the interaction between molecule and nanoantenna. The field radiated from the polarized molecule at a certain position (denoted by the index m) acts back on the molecule itself after interacting with the spherical nanoparticle. This interaction induces a self-consistent molecular dipole moment, which can be expressed via the self-interaction Green tensor $\vec{\vec{\mathbf{G}}}_{\text{mm}}$, as

$$\mathbf{p}_{\text{pol}} = \frac{\hat{\alpha}_{\text{mol}} \mathbf{E}^0_{\text{loc}}}{\vec{\vec{\mathbf{I}}} - \hat{\alpha}_{\text{mol}} \vec{\vec{\mathbf{G}}}_{mm}} \tag{4}$$

with $\vec{\vec{\mathbf{I}}}$ the unit matrix tensor (see section S2 of the Supporting Information for details). The modified self-consistent local electric field acting on the molecule can then be obtained from

$$\mathbf{E}_{\text{loc}} = \mathbf{E}^0_{\text{loc}} + \vec{\vec{\mathbf{G}}}_{mm} \mathbf{p}_{\text{pol}} \tag{5}$$

We consider next the spatial extension of the molecule in the buildup of the electronic dipolar transition. As described in the previous section, the key point is that the molecular electronic transition can be described as a summation of local dipole moments, $\delta\mu^{(m)}_{eg}$, thus we need to consider the different local electric fields, $\mathbf{E}^{(m)}_{\text{loc}}$, at the mth position of each of the local

https://dx.doi.org/10.1021/acs.jpcc.9b10256
J. Phys. Chem. C 2020, 124, 4674−4683

dipole moments to account for the full electromagnetic interaction. It is worthwhile to note that in order to account for the electromagnetic coupling of the molecular local dipoles with the antenna, the mutual interaction between dipoles is mediated exclusively via the nanoantenna, as the direct interaction between them is naturally accounted for within the ab initio calculations (the details can be found in section S2 of the Supporting Information).

The extinction spectra of the coupled system can be obtained from the coherent polarizations of nanoparticle and molecule, and are shown in parts e and f of Figure 2. We compare the results based on the assumption of a molecular point dipole (e), with those obtained with the use of the full quantum chemistry information on the molecular electronic states (f). When the molecular dipole is located at the center of the yz plane ($\delta z = 0$) at a distance d from the particle surface, the electromagnetic coupling between the local field and molecular dipole is negligible, therefore only the absorption from the metallic nanoparticle can be observed (blue line). As the molecule moves transversely (along the z direction, with δz = 0.1 nm), a clear Fano-like feature appears in the spectrum, as a consequence of an increasing coupling strength between the molecular dipole and plasmonic field. One can observe that although the spectral features are qualitatively similar for both the point-dipole description and the full quantum calculation, substantial quantitative differences emerge: the actual position of the Fano profile is shifted about 50 meV to a larger energy when the full quantum description of the molecule is considered, as a consequence of the spread of the electronic transition within the local field of the plasmonic nanoparticle. The contrast of the Fano spectral feature also differs in magnitude between the two approaches, becoming 2-fold larger for the full quantum description. These results point out the importance of considering the full quantum distribution of the electronic dipole at the molecule for an accurate and quantitative description of the spectral absorption of the coupled system.

Emission Properties of the Coupled Antenna-Molecule System. Once excited, the molecule acts as a radiative source and spontaneously emits to the surrounding environment. The nearby gold nanoparticle will play the role of a nanoantenna and will influence the spontaneous emission of the molecule by scattering the molecular dipolar emission and then reacting back on the molecular dipole, in a self-interaction process.[32,33] Following the procedure outlined in the previous section and in the Supporting Information, we apply our model of polarization of the full molecule to analyze this situation. The panels in Figure 3a show the distribution of the scattered field on the surfaces of the gold nanoparticle corresponding to the molecular transition $S_0 \rightarrow S_1$, at a fixed separation distance (d = 0.5 nm), with the molecule parallel to the closest particle surface, and for particles of different radius (R = 1, 5, and 10 nm). The panels in Figure 3b show the same situation for a molecular transition described within the point dipole approximation. Different from the situation of planewave illumination, as shown in Figure 2b, where mainly a dipolar surface plasmon is excited at the nanoparticle, when a dipole is located near the particle as a localized source of light, higher-order plasmonic modes are induced at the surface of the particle, particularly for large nanoparticles. The excited local plasmon mode is no longer a dipolar plasmon but a collection of multiple polarizations, also called "pseudomode".[6,34] As the size of the nanoparticle becomes smaller, the contribution of these higher-order plasmonic modes decreases, and the relative weight of the dipolar plasmonic mode recovers its strength.

We compare now the induced plasmonic fields at the nanoparticle when a full molecule and when a point dipole is considered. One can observe that the field distribution at the particle for the point-dipole excitation is more concentrated than that of the full molecular dipole, particularly when the size of the nanoparticle is comparable to the size of the ZnPc molecule (1−2 nm), as shown in parts a and b of Figure 3 for R = 1 nm (left panels). This is reasonable considering that the spatial distribution of the molecular transition dipole is much more spread than for a point dipole, indicating the limitation of the point−dipole approximation to describe this situation, and the importance of considering simultaneously the spatial distribution of photonics states, as well as that of the electronic states. Such a difference is more pronounced for smaller molecule−surface distance (see for example Figure S2 in section S3 of the Supporting Information). Even for a relatively large nanoparticle (R = 10 nm), the higher-order plasmonic fields induced at the particle are larger in the molecular point−dipole approximation, compared to the full molecular transition dipole, as shown in parts a and b of Figure 3 (right-hand panels).

In order to visualize the self-interaction in real space, we further plot the imaginary part of the self-consistent scattered field $\mathbf{E}_s$ at the molecular plane (yz-plane at a distance d = 0.5 nm away from the metal surface) in Figures 3, parts c and d for the same sizes of the nanoantenna considered above (R = 1 nm, 5 and 10 nm). As we discuss in the next section, the imaginary part of the scattered field determines the Purcell factor. The point dipole only interacts with the scattered field in the central point [upper panel of Figure 3c], whereas for the full molecular transition dipole, the spatial distribution of the electronic transition spreads over the atomic positions of the molecule [Figure 3d], determining the strength and extension of the self-interaction.

Purcell Factor and Lamb Shift. The enhancement of the molecular spontaneous emission, i.e., the Purcell factor, and the energy shift produced in the emission by the interaction with the plasmonic field, i.e., the Lamb shift, are important properties of an emitter located inside or near an optical resonator. Both quantities are only determined by the self-interaction of the molecule with the gold nanoparticle, regardless of the polarization conditions of the incident light. For a typical description of the emitter as a point-dipole, the imaginary part of the self-interaction, or interaction energy, given by the local field acting on the dipole as $\mu \cdot \mathbf{E}_s$, determines the total spontaneous decay rate of the emitter:

$$\gamma_{tot} = \frac{2}{\hbar}\mathrm{Im}\{\mu \cdot \mathbf{E}_s\} \tag{6}$$

and hence, the enhancement of the emission rate, or Purcell factor, F_P, can be estimated as[31]

$$F_P = \frac{\gamma_{tot}}{\gamma_0} = 1 + \frac{6\pi\varepsilon_0 c^3}{\omega^3}\frac{1}{|\mu|^2}\mathrm{Im}\{\mu \cdot \mathbf{E}_s\} \tag{7}$$

where γ_0 is the spontaneous emission in vacuum, ε_0 is the vacuum permittivity, and c is the speed of light in vacuum.

The real part of the self-reaction results in a shift of the resonant frequency of the molecule, $\delta\omega_L$, so-called the photonic Lamb shift. The Lamb shift is given by[24,35,36]

https://dx.doi.org/10.1021/acs.jpcc.9b10256
J. Phys. Chem. C 2020, 124, 4674−4683

$$\delta\omega_L = -\frac{1}{\hbar}\mathrm{Re}\{\boldsymbol{\mu}\cdot\mathbf{E}_s\} \tag{8}$$

To account for the spatial extension of the molecular electronic transition, the value of $\boldsymbol{\mu}\cdot\mathbf{E}_s$ is replaced by the sum of the contribution of each local dipole, $\sum_j \delta\boldsymbol{\mu}_{eg}^{(j)}\cdot\mathbf{E}_s^{(j)}$ in the expressions above.

We compare the values of the Purcell factor F_P and Lamb shift $\delta\omega_L$ of a molecular emitter in the presence of the spherical nanoantenna in parts a and b of Figure 4, respectively, as a function of the nanoparticle size (radius R from 0.5 to 50 nm). Two different molecule−surface separation distances are considered to activate different orders and strengths of plasmonic modes (d = 0.5 and 1.0 nm). For the shortest separation distance (d = 0.5 nm, red lines and symbols), the Purcell factor and Lamb shift obtained within the full quantum description of the molecule (squares) are generally smaller than those obtained within the point-dipole approximation (solid line). The full molecular dipole is more spread in space than the point dipole; therefore, the average electric field experienced by the entire molecule is smaller than for a point.

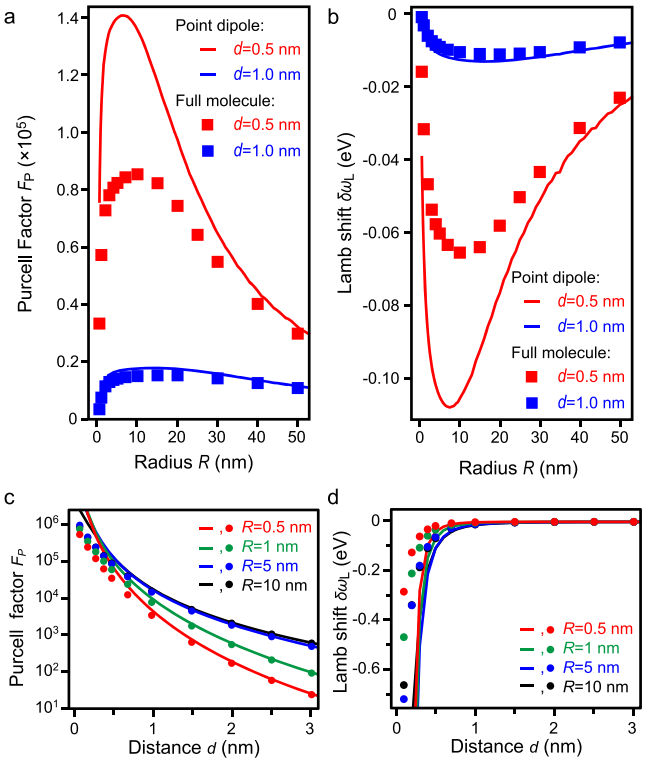

Figure 4. (a) Purcell factor of a ZnPc molecule in the presence of a spherical gold nanoparticle as a function of the nanoparticle size (radius R from 0.5 to 50 nm). Two different molecule−surface distances are considered, d = 0.5 nm (red) and 1.0 nm (blue). (b) Lamb shift for the same conditions as in (a). In parts a and b, the point−dipole description is displayed with solid lines, and results from the full chemical description of the molecule are displayed with squares. (c) Purcell factor and (d) Lamb shift of a ZnPc molecule as a function of the separation distance between molecule and particle surface. Different sizes of the nanoparticle are shown, with radius R = 0.5 nm (red), 1 nm (green), 5 nm (blue), and 10 nm (black). In parts c and d, the point−dipole description is displayed with solid lines, and results from the full chemical description of the molecule are displayed with dots.

As the size of the gold nanoparticle becomes larger, the inhomogeneity of the self-interaction field is smoothed and the molecular dipole can effectively be regarded as a point dipole (see the convergence of red squares and red lines for larger radius). Furthermore, if the distance between the molecule and the nanoparticle is increased (d = 1 nm, blue squares and lines), the difference between the full molecular dipole and the point dipole becomes negligible because the field experienced by the molecule is more homogeneous, independently of the particle size.

The dependence of the Purcell factor F_P and the Lamb shift $\delta\omega_L$ as a function of separation distance between molecular emitter and nanoparticle is studied in more detail in Figure 4, parts c and d, respectively. For large separation distances (d > 1 nm), the values of both F_P and $\delta\omega_L$ obtained from the full molecular model nicely coincide with those obtained within the point-dipole approximation for all the sizes of the plasmonic particles considered. This result clearly shows that a typical organic molecular emitter of about 1−2 nm in size can be accurately regarded as a point dipole for separation distances larger than its own size. However, considerable differences appear when the separation distance becomes shorter (d < 1 nm, as shown for d = 0.5 nm in Figure 4, parts a and b (red lines and squares)). The closer the distance between the molecule and the nanoparticle, the more the Purcell factor and Lamb shift depart from the values obtained with the point-dipole approximation. Consistent with the results in Figure 4, parts a and b, this difference for short separation distances is particularly pronounced for smaller nanoantenna sizes (R = 0.5 nm and R = 1 nm). The physical origin of the difference in the results between both models is ultimately related to the activation of either the plasmonic dipolar mode or higher-order modes in the nanoantenna, as discussed in the comparison of the fields scattered by the molecule on the particle surface (Figure 3, parts a and b). For a point dipole source, higher-order multiple modes are excited as long as the distance is close enough. For a full molecular dipole, because of the spatial extent of the molecular dipole, if the size of nanoparticle is comparable to the size of the molecule, then higher-order modes are less effectively excited even if the particle is very close to the molecule.

Total Light Emission Rate. The radiation rate γ_{rad} of the molecule-antenna system can be obtained from the calculation of the far field, integrated over all directions, as obtained for instance from Mie theory. Based on the radiation rate and on the excitation rate, the total light emission rate can be obtained as $\gamma_{em} = \gamma_{exc}Q = \gamma_{exc}(\gamma_{rad}/\gamma_{tot})$, where $Q = \gamma_{rad}/\gamma_{tot}$ is defined as the quantum yield. Here we consider a situation of resonant excitation of the system, thus a frequency of 2.28 eV is chosen for both excitation and emission processes.

We first consider the excitation rate γ_{exc} for a polarization of the incident light with the electric field along the z-axis parallel to the dipole moment of the molecular transition $S_0 \rightarrow S_1$. The value of γ_{exc} shows a different tendency with separation distance for a central position of the molecule (Figure 5a), and for a displaced lateral position with respect to the gold nanoparticle (Figure 5b). If the nanoparticle is located on top of the center of the molecule (z = 0 nm) and approaches to the molecule from d = 3.0 to 0.2 nm, the induced scattering field becomes stronger as the distance decreases, but the excitation rate decreases for R < 1 nm because of a cancellation between the incident and scattered fields (red and green lines and dots in Figure 5a). However, if the gold nanoparticle is shifted 1 nm

https://dx.doi.org/10.1021/acs.jpcc.9b10256
J. Phys. Chem. C 2020, 124, 4674−4683

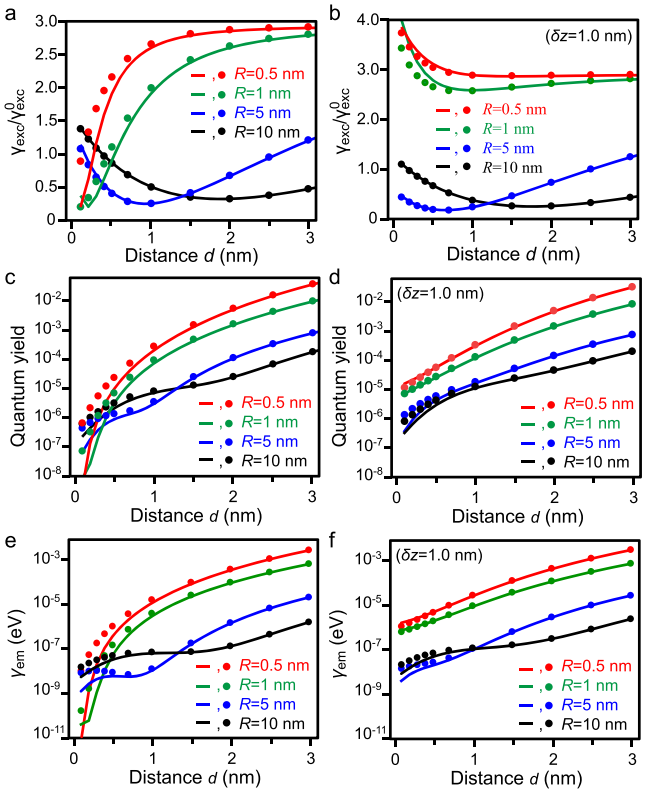

Figure 5. (a, b) Normalized excitation rate, (c, d) quantum yield, and (e, f) total emission rate of the ZnPc molecule as a function of molecule-particle surface separation distance for different nanoparticle radii, R = 0.5 nm (red), 1 nm (green), 5 nm (blue), 10 nm (black). In parts a, c, and e, the particle is on top of the center of the molecule, and in parts b, d, and f, the nanoparticle is displaced laterally 1 nm (δz = 1 nm) with respect to the center of the molecule. Results obtained with the point−dipole description of the molecule are displayed with solid lines, and those with the use of a full quantum chemistry description of the molecule are displayed with solid dots.

laterally, along the z-axis, which leaves the nanoparticle approximately on top of one of the lobes of the ZnPc molecule, the values of γ_{exc} generally increase as the molecule−surface separation distance d decreases (see Figure 5b). This occurs because the position of the nanoparticle, laterally displaced, breaks the symmetry of the system and in such a configuration, a more intense interaction of the molecular dipolar polarization and the particle local field is favored. For large nanoantennas and large molecule−particle surface distances, the results from the point−dipole approximation agree very well with those from the full quantum description of the molecular transition (compare solid lines and dots, respectively in Figure 5, parts a and b). However, for nanoantennas smaller than 1 nm, or separation distances smaller than 1 nm, which is approximately the size of the molecule, the two approximations provide different results. Depending on the actual size of the plasmonic nanoantenna, and the separation distance to the molecule, this difference can increase or reduce the value of the excitation rate (see additional calculations of excitation rates in Figure S3, section S4 of the Supporting Information).

Some of these trends can also be observed in the results of the quantum yield for the same configuration. The quantum yield of an emitter close to a spherical antenna is known to quench as the emitter gets closer to the surface of the nanoantenna.[3] This tendency can be observed in parts c and d of Figure 5 for different radii of the metallic nanoantenna, both for a position of the particle at the center of the molecule (Figure 5c) and for one displaced laterally on top of a molecular lobe (Figure 5d). The point−dipole approximation (solid lines) works very well for relatively large separation distances (d > 1 nm) and for the largest particles, whereas the full quantum description of the molecular structure (dots) provides different results for short separation distances and small particles. In such a situation, and for light excitation parallel to the molecule, as in this case, the full quantum description provides values of the quantum yield which could be even 1 order of magnitude larger. This behavior can be extrapolated to the emission rate of the molecule (see Figure 5, parts e and f), which is given by the product of the quantum yield and the excitation rate, as described above. These results show that the properties of emission of a molecular emitter can be often correctly captured by a point-dipole approximation, particularly in the presence of a homogeneous plasmonic field, however inhomogeneous fields with localizations below 1 nm, for example due to atomic protrusions, emphasize the importance of the chemical structure of the molecular emitter, in modifying relevant emission rates.

Fluorescence Microscopy. The chemical structure of a molecule is expected to influence the spatial symmetry of the properties of its light emission, even though often this connection might not be straightforward. The spatial distribution of the electronic states of the molecule can produce an asymmetry in the light emission process because the interaction between the molecule and nanoparticle is not isotropic, i.e., it changes as the plasmonic antenna moves around the molecule at a fixed distance from the center of the molecule. This asymmetry has been experimentally shown for the case of the ZnPc molecule[24] when a metallic tip is located around the molecule. In order to confirm the importance of the molecular chemical structure in the mapping of the molecule-antenna interaction, we consider the incident light polarized perpendicular to the molecular plane (along the x direction), as in typical STM configurations, and move the gold nanoparticle laterally over the ZnPc molecule while fixing the separation distance along the x axis at d = 0.5 nm. In this way, we analyze the spatial distribution of the radiation properties determined by the interaction with the nanoantenna. In all the calculations herein, both degenerate transition dipoles in the y and z directions of the ZnPc molecule have been taken into account. As shown in Figure 1c, the ZnPc molecule shows two degenerated orthogonal transition dipoles. Parts a−c of Figure 6 show the spatial maps of the normalized excitation rate, $\gamma_{exc}/\gamma^0_{exc}$, Purcell factor, F_P, and the total emission rate, γ_{em}, for the ZnPc molecular emitter coupled to the metallic nanoparticle located at the different positions. The upper panels show the results when the molecule is described as a point dipole, and the lower panels show the calculation of the same properties when the chemical structure of the molecule is properly considered. When the molecule is considered to be a point dipole, the overall radiation properties exhibit isotropic features in the yz plane. The Purcell factor reaches up to 10^5 in the center, while the maps of excitation and the emission rates show a doughnut-like structure resulting from the in-plane orientation of the transition dipoles. However, when the molecular structure of the molecule is properly accounted for, the rotational symmetry of the interaction with the emitter is broken and a

https://dx.doi.org/10.1021/acs.jpcc.9b10256
J. Phys. Chem. C 2020, 124, 4674−4683

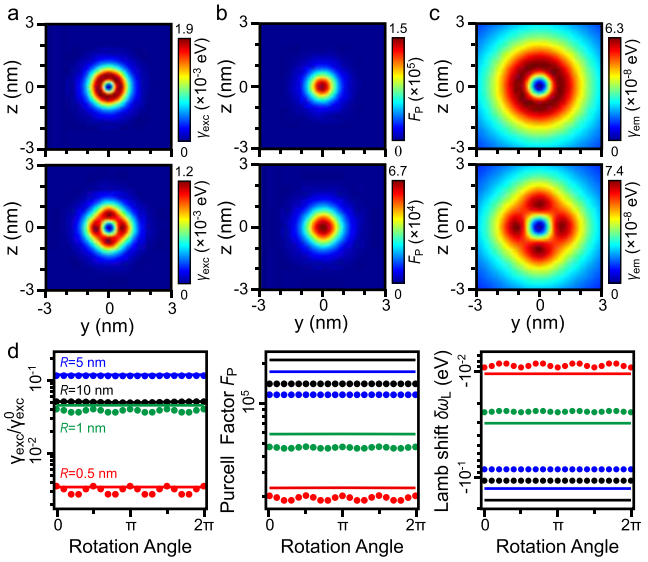

Figure 6. (a–c) Spatial maps of (a) normalized excitation rate $\gamma_{exc}/\gamma^0_{exc}$, (b) Purcell factor ($F_P$), and (c) total emission rate γ_{em} of a molecule close to a metallic nanoparticle within the point dipole model (top) and within the full molecule model (bottom), respectively. The dipole degeneracy in the x and y directions has been considered in all the maps. (d) Nanoparticle position-dependent excitation rate (left), Purcell factor (middle), and Lamb shift (right) for the gold nanoparticle located around the ZnPc molecule at a distance d = 0.5 nm and lateral distance of 1 nm, are shown for different gold nanoparticle radii: R = 0.5 nm (red), 1 nm (green), 5 nm (blue), and 10 nm (black) . The solid lines (−) represent the results within point dipole approximation and the dots (•) represent those within the model of the full molecular dipole.

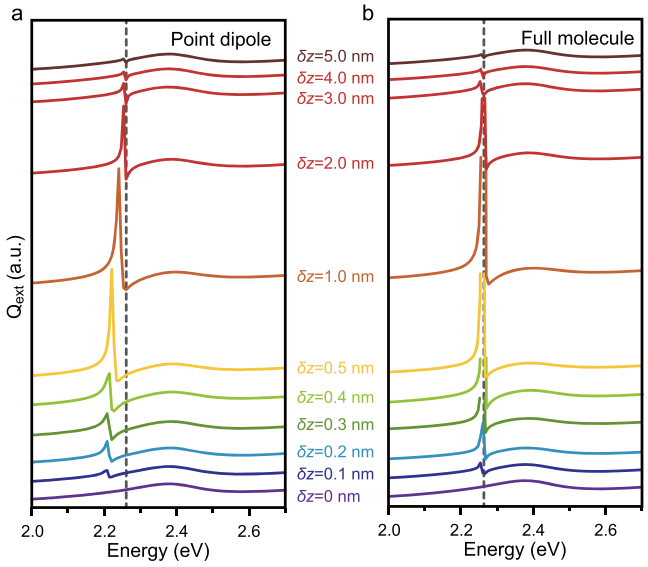

Figure 7. Evolution of the extinction spectra of the molecule-nanoantenna system for the point dipole approximation (a) and for the full molecule (b), respectively. The radius of the nanoparticle is R = 1 nm and the molecular position is d = 0.5 nm away from the surface on the yz plane. A relative lateral displacement between the nanoparticle and the dipole/molecular center along the transversal z-axis from δz = 0 to 5 nm is used to show the evolution of the spectral line shape. The molecular transition energy is indicated with dashed lines.

"four-lobe" symmetry of the excitation γ_{exc} rate, Purcell factor, and emission γ_{em} rate of the ZnPc molecule can be observed. Figure 6d shows the dependence of the excitation rate, the Purcell factor, and the Lamb shift on the size and position of the nanoantenna around the molecule. In this case, the gold nanoparticle is located on top of the molecule at a distance of d = 0.5 nm in the x direction, and at a fixed lateral distance of 1 nm from the center of the molecule. The variations of γ_{exc}, F_P, and $\delta\omega_L$ with a rotation angle from 0 to 2π around the molecule are consistent with the features shown in the spatial maps of Figure 6a–c. Within the point-dipole approximation, there is no observable change as the gold nanoparticle moves around the molecule, while for the full quantum chemical description of the molecule, periodic features related with the structural geometry of the ZnPc molecule can be observed. The spatial modulation of the excitation, Purcell factor, and Lamb shift is particularly relevant for gold nanoparticles of small size (red dots in Figure 6d). The corresponding values of the Purcell factor and Lamb shift ($F_P \sim 10^4$, $\delta\omega_L \sim$ 8–9 meV, varying within 2 meV) are consistent with the values of experimental results,[24] including the emergence of the modulation. These results show the importance of considering the chemical configuration of the molecule to address molecular spectroscopy in real space.

Spectroscopy of the Coupled System. Last, we address the spectral information on the molecule-antenna system, as a function of the nanoantenna lateral position on top of the molecule. Figure 7 shows the variation of the extinction spectra of the coupled nanoantenna–molecule system when the nanoantenna is displaced laterally away from the center of the molecule along the z-axis, with δz varying from 0 to 5 nm. As the particle moves away from the molecule, the position of the sharp Fano feature shifts with respect to the molecular frequency due to the Lamb shift. As shown in parts a and c of Figure 4, the point–dipole approximation overestimates the Lamb shift compared to the more accurate description of the dipole within the full quantum chemistry. On the other hand, because the full molecule has a more spread spatial distribution of electron densities than that given by the point dipole, in the case of a displaced lateral position of the nanoparticle with respect to the molecular dipole, the spectral signal and the apparent Fano line shape are enlarged when the particle is on top of the lobe of the molecule (see Figure 7b), as the interaction between molecule and plasmonic antenna field will be more effective in that position (see the enlargement of the Fano-feature and the maximum Lamb shift at δz = 0.5 nm in Figure 7b) than for a point dipole, which shows no spread of the electronic states when the particle is away from the center (see the smaller contrast of the Fano profile in Figure 7a). Moreover, if the nanoantenna is moved more than 3 nm away from the molecule (red lines in Figures 7, parts a and b), the point dipole and full molecular descriptions exhibit no significant differences, as the field distribution over the molecular structure becomes less inhomogeneous.

CONCLUSIONS

In summary, we have studied the importance of considering the chemical structure of a molecule in the correct description of its radiation properties when coupled to a small metallic particle acting as a nanoantenna. We have shown this with the canonical example of a molecular emitter such as ZnPc, located near a gold spherical nanoparticle. In most conditions, when the size of the nanoparticle and the distance between the molecule and the nanoantenna surface are larger than the size

https://dx.doi.org/10.1021/acs.jpcc.9b10256
J. Phys. Chem. C 2020, 124, 4674–4683

of the molecule, the molecular transition dipole can be accurately regarded as a point dipole. However, if the distance between molecular emitter and nanoantenna surface is smaller than about 1 nm, or the size of the nanoantenna is comparable to the spatial extent of the molecule, a more complete description of the molecular dipole within a quantum chemistry methodology is necessary. This description results in smaller values of the Purcell factor and Lamb shift as compared to the point−dipole description. Furthermore, a connection between the spatial distribution of the optical properties of the molecule and its chemical structure is found when the gold nanoparticle moves around the ZnPc molecule, revealing its "four-lobes" configuration. This information cannot be captured within the simpler point−dipole approximation. Our study provides a comprehensive review of the properties of radiation of a single molecular emitter in the presence of a plasmonic nanoantenna, and it shows the importance of considering the spatial structure of the molecular electronic states together with the distribution of the plasmonic states to properly address light emission from a molecule−nanoparticle system at the submolecular level.

■ ASSOCIATED CONTENT

Supporting Information

The Supporting Information is available free of charge at https://pubs.acs.org/doi/10.1021/acs.jpcc.9b10256.

Extra information on the electronic properties of the ZnPc molecule, theoretical details of the calculation of the excitation rate and the dipole moment of the full molecule modified by the self-interaction with the nanoparticle, additional calculations of the field scattered by the molecular dipole at short separation distances, and calculations of molecular excitation rates for antennas of different sizes (PDF)

■ AUTHOR INFORMATION

Corresponding Author

Javier Aizpurua − *Materials Physics Center, CSIC-UPV/EHU and Donostia International Physics Center (DIPC), Donostia-San Sebastián 20018, Spain;* orcid.org/0000-0002-1444-7589; Email: aizpurua@ehu.eus

Authors

Yao Zhang − *Materials Physics Center, CSIC-UPV/EHU and Donostia International Physics Center (DIPC), Donostia-San Sebastián 20018, Spain; Hefei National Laboratory for Physical Sciences at the Microscale and Synergetic Innovation Center of Quantum Information and Quantum Physics, University of Science and Technology of China, Hefei, Anhui 230026, China*

Zhen-Chao Dong − *Hefei National Laboratory for Physical Sciences at the Microscale and Synergetic Innovation Center of Quantum Information and Quantum Physics, University of Science and Technology of China, Hefei, Anhui 230026, China*

Complete contact information is available at: https://pubs.acs.org/10.1021/acs.jpcc.9b10256

Notes

The authors declare no competing financial interest.

■ ACKNOWLEDGMENTS

The authors express thanks for useful discussions with Tomas Neuman and Ruben Esteban. J.A. acknowledges Project IT1164-19 of the UPV/EHU research groups of the Basque Government and Project FIS2016-80174-P of the Spanish Ministry of Competitiveness and Innovation MINEICO.

■ REFERENCES

(1) Purcell, E. M. Spontaneous Emission Probabilities at Radio Frquencies. *Phys. Rev.* **1946**, *69*, 674.

(2) Itoh, T.; Yamamoto, Y. S.; Ozaki, Y. Plasmon-Enhanced Spectroscopy of Absorption and Spontaneous Emissions Explained Using Cavity Quantum Optics. *Chem. Soc. Rev.* **2017**, *46*, 3904−3921.

(3) Anger, P.; Bharadwaj, P.; Novotny, L. Enhancement and Quenching of Single-Molecule Fluorescence. *Phys. Rev. Lett.* **2006**, *96*, 113002.

(4) Becker, S. F.; Esmann, M.; Yoo, K. W.; Gross, P.; Vogelgesang, R.; Park, N. K.; Lienau, C. Gap-Plasmon-Enhanced Nanofocusing Near-Field Microscopy. *ACS Photonics* **2016**, *3*, 223−232.

(5) Trautmann, S.; Aizpurua, J.; Götz, I.; Undisz, A.; Dellith, J.; Schneidewind, H.; Rettenmayr, M.; Deckert, V. A Classical Description of Subnanometer Resolution by Atomic Features in Metallic Structures. *Nanoscale* **2017**, *9*, 391−401.

(6) Delga, A.; Feist, J.; Bravo-Abad, J.; Garcia-Vidal, F. J. Quantum Emitters near a Metal Nanoparticle: Strong Coupling and Quenching. *Phys. Rev. Lett.* **2014**, *112*, 253601.

(7) Bahsoun, H.; Chervy, T.; Thomas, A.; Börjesson, K.; Hertzog, M.; George, J.; Devaux, E.; Genet, C.; Hutchison, J. A.; Ebbesen, T. W. Electronic Light-Matter Strong Coupling in Nanofluidic Fabry-Pérot Cavities. *ACS Photonics* **2018**, *5*, 225−232.

(8) Schietinger, S.; Schröder, T.; Benson, O. One-by-One Coupling of Single Defect Centers in Nanodiamonds to High-Q Modes of an Optical Microresonator. *Nano Lett.* **2008**, *8*, 3911−3915.

(9) Hennessy, K.; Badolato, A.; Winger, M.; Gerace, D.; Atatüre, M.; Gulde, S.; Fält, S.; Hu, E. L.; Imamoglu, A. Quantum Nature of a Strongly Coupled Single Quantum Dot-Cavity System. *Nature* **2007**, *445*, 896−899.

(10) Pelton, M.; Aizpurua, J.; Bryant, G. Metal-nanoparticle plasmonics. *Laser Photonics Rev.* **2008**, *2*, 136−159.

(11) Chikkaraddy, R.; De Nijs, B.; Benz, F.; Barrow, S. J.; Scherman, O. A.; Rosta, E.; Demetriadou, A.; Fox, P.; Hess, O.; Baumberg, J. J. Single-Molecule Strong Coupling at Room Temperature in Plasmonic Nanocavities. *Nature* **2016**, *535*, 127−130.

(12) Li, R.-Q.; Hernángomez-Pérez, D.; García-Vidal, F. J.; Fernández-Domínguez, A. I. Transformation Optics Approach to Plasmon-Exciton Strong Coupling in Nanocavities. *Phys. Rev. Lett.* **2016**, *117*, 107401.

(13) Leng, H.; Szychowski, B.; Daniel, M.-C.; Pelton, M. Strong Coupling and Induced Transparency at Room Temperature with Single Quantum Dots and Gap Plasmons. *Nat. Commun.* **2018**, *9*, 4012.

(14) Baumberg, J. J.; Aizpurua, J.; Mikkelsen, M. H.; Smith, D. R. Extreme Nanophotonics from Ultrathin Metallic Gaps. *Nat. Mater.* **2019**, *18*, 668−678.

(15) Benz, F.; Schmidt, M. K.; Dreismann, A.; Chikkaraddy, R.; Zhang, Y.; Demetriadou, A.; Carnegie, C.; Ohadi, H.; De Nijs, B.; Esteban, R.; et al. Single-Molecule Optomechanics in "Picocavities. *Science* **2016**, *354*, 726−729.

(16) Zhang, R.; Zhang, Y.; Dong, Z. C.; Jiang, S.; Zhang, C.; Chen, L. G.; Zhang, L.; Liao, Y.; Aizpurua, J.; Luo, Y.; et al. Chemical Mapping of a Single Molecule by Plasmon-Enhanced Raman Scattering. *Nature* **2013**, *498*, 82−86.

(17) Rivera, N.; Kaminer, I.; Zhen, B.; Joannopoulos, J. D.; Soljačić, M. Transitions on the Atomic Scale. *Science* **2016**, *353*, 263−269.

(18) Liu, P.; Chulhai, D. V.; Jensen, L. Single-Molecule Imaging Using Atomistic Near-Field Tip-Enhanced Raman Spectroscopy. *ACS Nano* **2017**, *11*, 5094−5102.

(19) Urbieta, M.; Barbry, M.; Zhang, Y.; Koval, P.; Sánchez-Portal, D.; Zabala, N.; Aizpurua, J. Atomic-Scale Lightning Rod Effect in Plasmonic Picocavities: A Classical View to a Quantum Effect. *ACS Nano* **2018**, *12*, 585−595.
(20) Shin, H.-H.; Yeon, G. J.; Choi, H.-K.; Park, S.-M.; Lee, K. S.; Kim, Z. H. Frequency-Domain Proof of the Existence of Atomic-Scale SERS Hot-Spots. *Nano Lett.* **2018**, *18*, 262−271.
(21) Lee, J.; Crampton, K.; Tallarida, N.; Apkarian, V. Visualizing Vibrational Normal Modes of a Single Molecule with Atomically Confined Light. *Nature* **2019**, *568*, 78−82.
(22) Kern, J.; Großmann, S.; Tarakina, N. V.; Häckel, T.; Emmerling, M.; Kamp, M.; Huang, J. S.; Biagioni, P.; Prangsma, J. C.; Hecht, B. Atomic-Scale Confinement of Resonant Optical Fields. *Nano Lett.* **2012**, *12*, 5504−5509.
(23) Zhang, Y.; Luo, Y.; Zhang, Y.; Yu, Y. J.; Kuang, Y. M.; Zhang, L.; Meng, Q. S.; Luo, Y.; Yang, J. L.; Dong, Z. C.; et al. Visualizing Coherent Intermolecular Dipole-Dipole Coupling in Real Space. *Nature* **2016**, *531*, 623−627.
(24) Zhang, Y.; Meng, Q. S.; Zhang, L.; Luo, Y.; Yu, Y. J.; Yang, B.; Zhang, Y.; Esteban, R.; Aizpurua, J.; Luo, Y.; et al. Sub-Nanometre Control of the Coherent Interaction between a Single Molecule and a Plasmonic Nanocavity. *Nat. Commun.* **2017**, *8*, 15225.
(25) Imada, H.; Miwa, K.; Imai-Imada, M.; Kawahara, S.; Kimura, K.; Kim, Y. Single-Molecule Investigation of Energy Dynamics in a Coupled Plasmon-Exciton System. *Phys. Rev. Lett.* **2017**, *119*, 013901.
(26) Doppagne, B.; Chong, M. C.; Lorchat, E.; Berciaud, S.; Romeo, M.; Bulou, H.; Boeglin, A.; Scheurer, F.; Schull, G. Vibronic Spectroscopy with Submolecular Resolution from STM-Induced Electroluminescence. *Phys. Rev. Lett.* **2017**, *118*, 127401.
(27) Neuman, T.; Esteban, R.; Casanova, D.; García-Vidal, F. J.; Aizpurua, J. Coupling of Molecular Emitters and Plasmonic Cavities beyond the Point-Dipole Approximation. *Nano Lett.* **2018**, *18*, 2358−2364.
(28) Nafie, L. A. Electron Transition Current Density in Molecules. 1. Non-Born-Oppenheimer Theory of Vibronic and Vibrational Transitions. *J. Phys. Chem. A* **1997**, *101*, 7826−7833.
(29) Freedman, T. B.; Gao, X.; Shih, M. L.; Nafie, L. A. Electron Transition Current Density in Molecules. 2. Ab Initio Calculations for Electronic Transitions in Ethylene and Formaldehyde. *J. Phys. Chem. A* **1998**, *102*, 3352−3357.
(30) Sakurai, J. J.; Tuan, S. F. *Modern quantum mechanics*; Addison-Wesley: 2004.
(31) Novotny, L.; Hecht, B. *Principles of Nano-Optics*, 2nd ed.; Cambridge University Press: 2012.
(32) Senitzky, I. R. Radiation-Reaction and Vacuum-Field Effects in Heisenberg-Picture Quantum Electrodynamics. *Phys. Rev. Lett.* **1973**, *31*, 955−958.
(33) Wylie, J. M.; Sipe, J. E. Quantum Electrodynamics near an Interface. *Phys. Rev. A: At., Mol., Opt. Phys.* **1984**, *30*, 1185−1193.
(34) Li, R. Q.; Hernángomez-Pérez, D.; García-Vidal, F. J.; Fernández-Domínguez, A. I. Transformation Optics Approach to Plasmon-Exciton Strong Coupling in Nanocavities. *Phys. Rev. Lett.* **2016**, *117*, 107401.
(35) Yao, P.; Van Vlack, C.; Reza, a.; Patterson, M.; Dignam, M. M.; Hughes, S. Ultrahigh Purcell Factors and Lamb Shifts in Slow-Light Metamaterial Waveguides. *Phys. Rev. B: Condens. Matter Mater. Phys.* **2009**, *80*, 195106.
(36) D'Agostino, S.; Alpeggiani, F.; Andreani, L. C. Strong Coupling between a Dipole Emitter and Localized Plasmons: Enhancement by Sharp Silver Tips. *Opt. Express* **2013**, *21*, 27602.

https://dx.doi.org/10.1021/acs.jpcc.9b10256
J. Phys. Chem. C 2020, 124, 4674−4683